

Robust synchronization in fiber laser arrays

Slaven Peleš*

Center for Nonlinear Science and School of Physics, Georgia Institute of Technology, Atlanta, Georgia 30332-0430, USA

Jeffrey L. Rogers†

HRL Laboratories, LLC, Malibu, California 90265, USA

Kurt Wiesenfeld‡

Center for Nonlinear Science and School of Physics, Georgia Institute of Technology, Atlanta, Georgia 30332-0430, USA

(Received 21 September 2005; published 17 February 2006)

Synchronization of coupled fiber lasers has been reported in recent experiments [Bruesselbach *et al.*, *Opt. Lett.* **30**, 1339 (2005); Minden *et al.*, *Proc. SPIE* **5335**, 89 (2004)]. While these results may lead to dramatic advances in laser technology, the mechanism by which these lasers synchronize is not understood. We analyze a recently proposed [Rogers *et al.*, *IEEE J. Quantum Electron.* **41**, 767 (2005)] iterated map model of fiber laser arrays to explore this phenomenon. In particular, we look at synchronous solutions of the maps when the gain fields are constant. Determining the stability of these solutions is analytically tractable for a number of different coupling schemes. We find that in the most symmetric physical configurations the most symmetric solution is either unstable or stable over insufficient parameter range to be practical. In contrast, a lower symmetry configuration yields surprisingly robust coherence. This coherence persists beyond the pumping threshold for which the gain fields become time dependent.

DOI: [10.1103/PhysRevE.73.026212](https://doi.org/10.1103/PhysRevE.73.026212)

PACS number(s): 05.45.Xt, 42.55.Wd, 05.45.-a

I. INTRODUCTION

Synchronization of groups of interacting dynamical subsystems has been studied in a wide range of contexts from sociology to biology, chemistry, and physics [1,2]. Animal gaits, cardiac rhythms, and hormonal cycles serve as biological examples. In physical systems, examples include electronic beam steering [3–5], power combining of Josephson junctions, nanoelectromechanical systems [6], and encrypted communication. For these and other applications there now exists an extensive literature studying the properties of mathematical model systems to capture the essence of the observed synchronization [7]. Applying these findings to new applications can, and often does, reveal unexpected aspects of the underlying phenomenon. The focus of this paper is one such example: the role of symmetry in power combining of lasers.

Conceptually a system of coupled subsystems can be separated into the internal dynamics of each member and the architecture which connects them [8,9]. Mathematically the behavior of the individual subsystems is defined by differential equations or iterative maps, while the connectivity is formulated as a graph where nodes represent the subsystems and edges define couplings. In this formulation the notion of symmetry can be applied to both of the system concepts. Symmetries of the differential equations reflect similarities in the subsystem properties (for example, the subsystems may be identical copies), while on the graph symmetries appear

as the freedom to permute elements, coupling magnitude uniformity, or consistency in the number of neighbors.

We will investigate the role of system symmetries in the formation of symmetric solutions by studying the existence and stability of the inphase state in a recently proposed model for laser arrays [10]. We will provide a detailed analysis of the stability of a highly symmetric solution that is of significant interest in applications. Our stability analysis will show that the stability of this symmetric solution is enhanced by the reduction of specific system symmetries.

In optics, power combining is an area where a synchronization based approach offers a number of attractive advantages over conventional methods. Often single monolithic sources face physical limitations that may be avoided by using an array. For one, array components may be operated at lower power levels where they may be more efficient and have favorable physical properties, including effective heat dissipation and reliability. Additionally, there is the possibility that no active control will be required. Aside from reducing the array complexity a completely passive system is not limited by the relatively fast optical time scales that an active control approach must address.

Synchronization offers a number of additional advantages to the array architecture. To produce optimal brightness from the array the in-phase solution, where all the sources have the same frequency and phase, is desirable. The in-phase state is a highly symmetrical solution that is attractive because the brightness, or peak intensity, produced increases as the square of the number of lasers (N^2). Another beneficial aspect of this dramatic growth is that the beam width decreases as $1/N$. Thereby the inphase solution has both optimal brightness and is self-focusing in the far field. Due to manufacturing variations, fluctuations in temperature, and external noise sources a group of lasers will possess some

*Electronic address: slaven.peles@physics.gatech.edu†Electronic address: jeff@hrl.com‡Electronic address: kurt.wiesenfeld@physics.gatech.edu

distribution in lasing frequencies that may vary in time. Synchronization offers an approach to overcoming these intrinsic differences and forming the inphase state without requiring active control.

A decade after the demonstration of a working laser by Maiman in 1960 [11] arrays were proposed to address coherence problems with junction lasers [12]. Broad contact versions of these lasers showed a breakdown in spatial and temporal coherence due to multiple lasing filaments (pathways). Arrays of coupled single filament stripe lasers were then proposed as a solution. Combining of laser output from an array has remained an active area of research.

A significant milestone in these efforts was recently achieved when several experiments demonstrated spontaneous in-phase states in small groups of fiber lasers [13–18]. While these findings may one day lead to a host of new devices, the experiments also displayed a number of features indicating the underlying mechanisms are poorly understood. This understanding gap was further manifested in the variety of descriptions used to interpret the laboratory results. At least one series of experiments [13,14,18], based on general principles from nonlinear sciences, interpreted findings in terms of mutual synchronization and self-organization. These experiments helped motivate our analysis.

Fiber lasers are known to exhibit rich dynamical behavior such as period doubling bifurcations [19], chaos [20], and self-mode locking [21]. Modeling the dynamics of a single fiber only is already a challenging task [22–25]. So far several models for coupled fiber laser structures have been proposed in an attempt to explain self-organizing phenomena seen in the experiments. Those include the model for hexagonal multicore fibers [26] and for two coupled fiber lasers [27].

As a next step towards understanding spontaneous synchronization in fiber laser arrays we recently proposed a model [10] that, while initially leaving out some aspects of the experimental systems, nevertheless captures key dynamical features observed in the laboratory [13,14].

In this paper we use this model to investigate the existence and stability of the in-phase state in laser arrays. The model is valid over a range of gain magnitudes, including the relatively high gain associated with rare-earth doped fiber lasers, where the usual assumptions behind models using ordinary differential equations break down. We augment the analytic stability analysis with numerical simulations to investigate the robustness of the solutions as well as what happens at higher pump values where the output intensity switches from constant values to pulsing behavior. In the cases we have studied, the conclusions regarding stability and robustness of in-phase states remain true even into the pulsed-intensity regime.

We find that the stability of the in-phase solution is enhanced by reducing the symmetry of the physical array. Four architectures are analyzed in order of decreasing symmetry. First, the all-to-all coupled array of identical lasers is studied. In this case, where there is full permutation symmetry, the in-phase solution is stable over a relatively small range of parameters. Next we reduce the symmetry to cyclic permutations by considering a ring of identical lasers with nearest neighbor interactions. In this case no stable in-phase solution

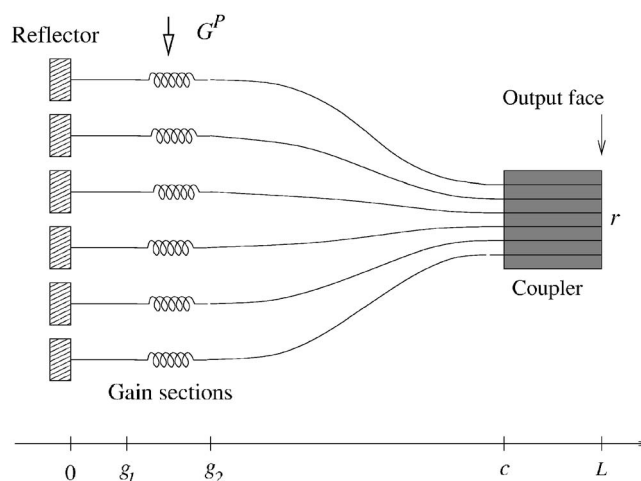


FIG. 1. Schematic of the laser array. The coupler is enlarged for clarity; in a typical experimental setup it makes less than one percent of the cavity length.

exists. Third, a laser is added to the middle of a ring of six elements to form a triangular lattice of identical lasers with nearest neighbor interactions. This breaks full cyclic permutation symmetry since the middle laser has a different number of neighbors, and the in-phase solution is found to be marginally stable to linear order. Finally, for the seven element array with nearest neighbor interactions on a triangular lattice one of the lasers is allowed to be nonidentical. Introducing a difference in this one array element, a strategy inspired by laboratory observations [14], has the result of stabilizing the in-phase solution; moreover, the in-phase solution is robust in the sense that it is attracting for typical initial conditions. Thereby, reducing the physical symmetry of the array has the effect of stabilizing a highly symmetric solution. Conveniently, this solution is of significant interest in applications.

II. BACKGROUND

We study an array of several fiber lasers, which are coupled near the output end as shown in Fig. 1. Each laser cavity is terminated by a near 100% reflector at one end, and the coupler output face at the other. The fiber lasers have separate gain sections, and do not interact with each other outside the coupler. The output face of the coupler is cleaved so that the reflection coefficient is the same for each fiber. The optical fiber field reflection coefficient is only around 20% (i.e., 4% of intensity), so the lasers have to operate in a high gain regime.

The equations of motion for a single axial mode in this system can be written in the form of an iterated map [10,28]:

$$E'_n = A_{nm} E_m, \quad (1)$$

$$G'_n = G_n + \epsilon(G_n^p - G_n) - \frac{2\epsilon}{I_{\text{sat}}}(1 - e^{-G_n})|E_n|^2, \quad (2)$$

where each iteration propagates the system by one cavity round trip time T , i.e., the time it takes for one back and forth

cycle. Here, A is the round trip field evolution operator, G_n is the gain of the n th fiber, G_n^p is the pump parameter for the n th fiber, and I_{sat} is the saturation parameter. The parameter ϵ is the ratio of the round trip and fluorescence times, which we assume is a small number: for the fiber lasers studied in recent experiments $\epsilon \sim 10^{-4}$ [10,13,14]. Equations (1) and (2) can be put in dimensionless form by expressing the fields E_n in units of $\sqrt{I_{sat}}$. The iterated map description is valid as long as the gain fields G_n change slowly with respect to the roundtrip time, or in other words for as long as $\epsilon G_n^p \ll 1$ is satisfied. Since ϵ is proportional to the fiber length, this condition sets a limit to the fiber length. The model is valid for a number of physically interesting situations. As an illustration, for typical rare earth doped fibers pumped about ten times the lasing threshold, the map description is valid for fiber lengths up to the order of hundreds of meters. A detailed discussion on this model is given in Ref. [10].

One cavity roundtrip can be separated in two main stages: (i) Light propagates from the coupler input ($z=c$) to the partially reflecting output face ($z=L$), bounces off the output face and propagates back to the coupler input. During this stage the fields in individual fibers interact with each other. (ii) Light propagates through separate fibers from the coupler input toward the reflector ($z=0$), bounces off, and propagates back to the coupler input. During this stage the noninteracting fields get amplified at each pass through the gain sections ($g_1 < z < g_2$).

The roundtrip operator A can be written as a product of field evolution operators for each stage of the roundtrip. In our case it can be represented by a matrix with elements

$$A_{nm} = r e^{G_n + i\phi_n} S_{nm}. \quad (3)$$

Here S is the coupling matrix, which describes field propagation back and forth through the coupling region ($c < z < L$), ϕ_n is the phase that field in n th fiber acquires outside of the coupling region ($0 < z < c$), e^{G_n} is the field amplification during two passes (once each way) through the gain section of the n th fiber ($g_1 < z < g_2$), and r is the field reflection coefficient at the output face. In what follows, we set the ϕ_n equal to zero.

In this paper, we choose the reference plane at the base of the coupler ($z=c$) instead of the output face ($z=L$) as chosen in Ref. [10]. As a consequence the form of Eq. (3) is simplified with S_{nm} being the coupling matrix for two passes through the coupler instead of one. We stress that any point along the z axis may be chosen as the reference plane. The fields at the output face are related to those at the input face by a constant linear transformation; consequently, if the input fields are coherent then so are the fields at the output face. Furthermore, for the symmetric couplers we will consider, the particular phase relationships are also preserved.

An essential part of the array architecture is the coupling between the fibers. We describe here a general formulation of passive linear coupling between fiber lasers. The particular coupling scheme we consider was originally motivated by optical waveguide couplers, but the resulting equations hold more generally, as long as the coupling is small compared to propagation constants of individual fibers. In a typical cou-

pler a certain amount of light leaks from one fiber core into another. This is known as fiber cross talk. It is difficult to obtain an accurate description of field mixing in a realistic coupler. However, simplified treatments exist, which can provide reasonable estimates [29,30]. A freely propagating field in an optical fiber satisfies a plane wave equation

$$\frac{dE_n}{dz} - i\beta_n E_n = 0, \quad (4)$$

where β_n is the propagation constant. The loss in the fiber can be incorporated as the imaginary part of the propagation constant, so that $\beta_n = \beta_n^r + i\beta_n^i$, and $\beta_n^i > 0$. When the fibers are coupled, the field in fiber j acts as a perturbation to the field in fiber n , so the equation for E_n inside the coupler can be written as

$$\frac{dE_n}{dz} - i\beta_n E_n = i \sum_{j \neq n} C_{nj} E_j. \quad (5)$$

This is true for any two fibers in the coupler, so we can write Eqs. (5) in the matrix form as

$$\frac{d\mathbf{E}}{dz} = i\mathbf{M}\mathbf{E}, \quad (6)$$

where $M_{kk} = \beta_k$, and $M_{kl} = C_{kl}$, for $k \neq l$. The propagation and coupling constants may be evaluated from physical properties of the coupler [29]. Matrix S , which appears in Eq. (3), then can be obtained by integrating Eq. (6) along the coupling region—that is, back and forth over the physical length of the coupler. At this point we shall make a couple of simplifying assumptions. We shall assume that coupling between two fibers is the same in both directions, and therefore M is symmetric. Also we shall assume that the coupler is uniform, so that M does not depend on z over its length. The expression for S then has the simple form

$$S = e^{iMd} e^{iM^T d} = e^{2iMd}, \quad (7)$$

where $d=L-c$ is the length of the coupler [31].

Before turning to the array calculations, it is useful to recap the behavior of the single fiber problem ($N=1$) [10]. There are two fixed point solutions, an off state ($G=G^p$, $E=0$) and an on state,

$$\tilde{G} = \ln(1/r), \quad |\tilde{E}|^2 = \frac{G^p - \ln(1/r)}{2(1-r)}. \quad (8)$$

Stability analysis of the fixed point reveals two transition points. The first is a transcritical bifurcation that occurs at the pumping level,

$$G_{tc}^p = \ln(1/r), \quad (9)$$

where the off state and the on state exchange stability. Then, at the pumping level

$$G_h^p = \ln(1/r) + \frac{1-r}{2-3r} \quad (10)$$

the system undergoes a Hopf bifurcation: as G^p is increased past G_h^p the fixed point Eq. (8) becomes unstable, and a stable quasiperiodic orbit is created. The gain field behaves

as a relaxation oscillator, and the laser operates in a pulsed mode. For reflection coefficient $r=0.187$, which we shall use in our numerical calculations, $G_{ic}^P=1.68$ and $G_h^P=2.24$.

III. STABILITY ANALYSIS OF CONSTANT GAIN SOLUTIONS: GENERAL CONSIDERATIONS

In the following sections we explore the existence and stability of synchronized states that are phase coherent. Our analysis focuses on constant gain solutions. These are both analytically tractable and can provide insight into the array dynamics even when the gain develops time dependence. Constant gain solutions correspond to continuous wave lasing, while time-dependent gains are characteristic of more complicated intensity states like pulsing.

Our analytic calculations test the linear asymptotic stability of certain highly coherent solutions. Thus we rigorously characterize the stability with respect to arbitrary but (infinitesimally) small perturbations in the electric fields and gain fields. Identifying the base solutions requires solving the full nonlinear equations for the model given by Eqs. (1) and (2), while the evolution equations for the perturbations are linear. The latter may be written in matrix form and the stability problem amounts to finding the eigenvalues of the $3N \times 3N$ evolution matrix. We exploit the system symmetries to block diagonalize this matrix, typically into 3×3 blocks, which greatly simplifies the problem. Of course, the application of linear stability to study laser arrays is not new [32]. An unusual aspect of the present problem is that the governing equations are iterative maps rather than differential equations.

The block reduction of the linear stability problem leads us to a thorough understanding of the asymptotic stability properties of highly coherent solutions with respect to infinitesimal perturbations. We augment these analytic results with numerical simulations in order to explore the effect of finite perturbations.

An essential ingredient determining the existence and stability of coherent solutions is how the elements are coupled. We consider three natural coupling configurations, in order of decreasing symmetry: (i) all-to-all coupling, (ii) nearest neighbor coupling on a ring, and (iii) a hexagonal star configuration.

Before turning to explicit calculations for each of these cases, we collect some valuable technical results which will be generally useful. For the moment, let us suppose only that $(\tilde{E}_n, \tilde{G}_n)$ is a solution to the governing Eqs. (1) and (2), and denote small deviations from this solution by $\eta_n = E_n - \tilde{E}_n$ and $\gamma_n = G_n - \tilde{G}_n$. These deviations evolve according to the linearized equation

$$\eta'_n = re^{\tilde{G}_n} \sum_m S_{nm} \eta_m + re^{\tilde{G}_n} \gamma_n \sum_m S_{nm} \tilde{E}_m,$$

$$\eta_n^* = re^{\tilde{G}_n} \sum_m S_{nm}^* \eta_m^* + re^{\tilde{G}_n} \gamma_n \sum_m S_{nm}^* \tilde{E}_m^*,$$

$$\gamma'_n = \gamma_n - \epsilon(1 + 2e^{-\tilde{G}_n} |\tilde{E}_n|^2) \gamma_n - 2\epsilon(1 - e^{-\tilde{G}_n}) (\tilde{E}_n \eta_n^* + \tilde{E}_n^* \eta_n). \quad (11)$$

If the coupling matrix S is circulant (i.e., every row of the matrix is a cyclic permutation of the row before [33]), it can be diagonalized by a unitary transformation $U^* S U$, where

$$U_{kl} = \frac{1}{\sqrt{N}} e^{-i2\pi kl/N}. \quad (12)$$

Moreover, the eigenvalues of S are

$$\lambda_n = \sum_{k=0}^{N-1} S_{0k} e^{-i2\pi nk/N}, \quad (13)$$

with associated eigenvectors $\mathbf{y}^{(n)} = (1, e^{-i2\pi n/N}, e^{-i4\pi n/N}, \dots, e^{-i2\pi(N-1)n/N})^T$, where the superscript T denotes transpose. If we now define variables

$$\psi_n = \frac{1}{\sqrt{N}} \sum_{k=0}^{N-1} \eta_k e^{i2\pi nk/N}, \quad (14)$$

$$\chi_n = \frac{1}{\sqrt{N}} \sum_{k=0}^{N-1} \eta_k^* e^{i2\pi nk/N}, \quad (15)$$

$$g_n = \frac{1}{\sqrt{N}} \sum_{k=0}^{N-1} \gamma_k e^{i2\pi nk/N} \quad (16)$$

the linearized problem Eqs. (11) can be written in block diagonal form with N sets of three coupled equations,

$$\psi'_n = re^{\tilde{G}_n} \lambda_n \psi_n + re^{\tilde{G}_n} g_n \sum_m S_{nm} \tilde{E}_m, \quad (17)$$

$$\chi'_n = re^{\tilde{G}_n} \lambda_n^* \chi_n + re^{\tilde{G}_n} g_n \sum_m S_{nm}^* \tilde{E}_m^*, \quad (18)$$

$$g'_n = [1 - \epsilon(1 + 2e^{-\tilde{G}_n} |\tilde{E}_n|^2)] g_n - 2\epsilon(1 - e^{-\tilde{G}_n}) \tilde{E}_n^* \psi_n - 2\epsilon(1 - e^{-\tilde{G}_n}) \tilde{E}_n \chi_n. \quad (19)$$

Thus far we have assumed only that the coupling matrix S is circulant. Things simplify further if we consider strictly in-phase solutions. In particular, suppose the assumed base solutions are

$$\tilde{E}_n = R_n e^{-i\omega t}, \quad \tilde{G}_n = \ln(1/r) \quad \text{for all } n, \quad (20)$$

where ω is real and t is the number of iterations. The solution (20) can be extended to continuous time in a natural way as shown in Fig. 2. If all fibers are equally pumped ($G_n^P = G^P$), then Eq. (2) implies that the amplitudes R_n are equal, and

$$R_n^2 = R^2 = \frac{G^P - \ln(1/r)}{2(1-r)}. \quad (21)$$

By substituting the assumed solution Eq. (20) into Eq. (1) we find that it exists provided $e^{-i\omega}$ is an eigenvalue of S for eigenvector $\mathbf{y}^{(0)} = (1, 1, \dots, 1)^T$. In other words

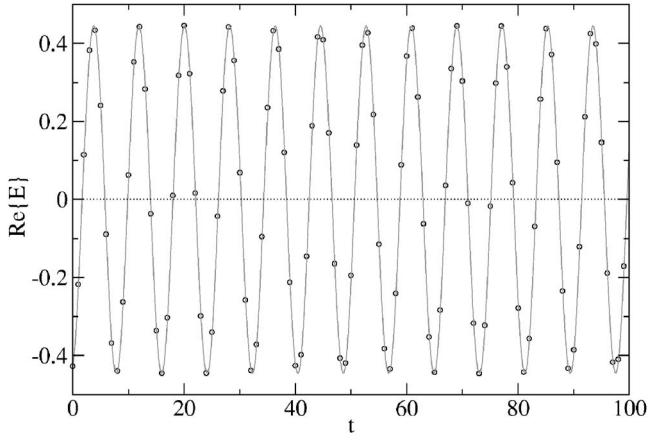


FIG. 2. In-phase solution for the all-to-all coupled fiber laser array (Sec. IV). The diagram shows the real part of the electric field vs time. The points represent map iterations obtained numerically and the solid line is the analytical solution (20) extended to continuous time.

$$e^{-i\omega} = \sum_m S_{nm} \text{ for all } n. \quad (22)$$

If S is circulant, the sum of the elements in each of its rows is the same. If S is furthermore unitary, its eigenvalues lie on the unit circle, and therefore condition Eq. (22) is satisfied [34]. If we substitute the base solution Eq. (20) in the linearized equations, we find

$$\psi'_n = \lambda_n \psi_n + R e^{-i\omega(t+1)} g_n, \quad (23)$$

$$\chi'_n = \lambda_n^* \chi_n + R e^{i\omega(t+1)} g_n, \quad (24)$$

$$g'_n = -2\epsilon(1-r)R e^{i\omega t} \psi_n - 2\epsilon(1-r)R e^{-i\omega t} \chi_n + [1 - \epsilon(1 + 2rR^2)]g_n. \quad (25)$$

We can remove the explicit time dependence of the Jacobi matrix by introducing another coordinate change

$$\psi_n = e^{-i\omega t} u_n, \quad \chi_n = e^{i\omega t} v_n. \quad (26)$$

Since from Eq. (22) it follows that for the in-phase solution $\lambda_0 = e^{-i\omega}$, we can write the linearized equations a

$$u'_n = (\lambda_n/\lambda_0)u_n + Rg_n,$$

$$v'_n = (\lambda_n/\lambda_0)^* v_n + Rg_n,$$

$$g'_n = -2\epsilon(1-r)Ru_n - 2\epsilon(1-r)Rv_n + [1 - \epsilon(1 + 2rR^2)]g_n. \quad (27)$$

The details of any particular coupling geometry ultimately determine the coupling matrix S and its eigenvalues λ_n . The eigenvalues of the first block are, however, independent of the geometry, because the matrix

$$J_0 = \begin{pmatrix} 1 & 0 & R \\ 0 & 1 & R \\ -2\epsilon(1-r)R & -2\epsilon(1-r)R & 1 - \epsilon(1 + 2rR^2) \end{pmatrix}$$

does not depend on the coupling constants. In fact, J_0 is just the Jacobi matrix for a single fiber laser in the on state. We therefore arrive at our first important conclusion: for a circulant coupling scheme a stable continuous wave in-phase solution may occur only within the same pumping range where the on state of a single fiber laser is stable—that is $G_{tc}^P < G^P < G_h^P$.

IV. ALL-TO-ALL COUPLING

For all-to-all coupling, each laser is coupled to all others with equal strength. The all-to-all coupling generator matrix M can be written as $M_{nm} = \beta\delta_{nm} + \kappa(1 - \delta_{nm})$, where δ is the Kronecker symbol, β is a propagation constant, and κ is the coupling constant between two fibers [29]. The coupling matrix is $S = \exp(i2Md)$ where d is the length of the coupler. We see that S is circulant, so the full reduction to Eqs. (27) may be made. The matrix M can be diagonalized using transformation Eq. (12), and therefore so can S ,

$$(U^* S U)_{nm} = (e^{i2dU^* M U})_{nm} = e^{i2d[\beta - \kappa + \kappa N \delta_{n,0}]} \delta_{nm}. \quad (28)$$

The eigenvalues of S are readily read off,

$$\lambda_n = e^{i2d[\beta - \kappa + \kappa N \delta_{n,0}]}. \quad (29)$$

There are $N-1$ degenerate eigenvalues of S , and hence there are infinitely many constant gain solutions to Eqs. (1) and (2) in the case of uniform all-to-all coupling. The in-phase solution is the only nondegenerate eigenvector of S . Its eigenvalue is $\lambda_0 = e^{-i\omega}$, and the frequency of the in-phase solution is

$$\omega = -2d[\beta + (N-1)\kappa]. \quad (30)$$

By applying the inverse transformation of Eq. (28) we obtain the analytical expression for coupling matrix elements given in terms of propagation constants and coupling coefficients:

$$S_{nm} = [U(U^* S U)U^*]_{nm} = \frac{1}{N} e^{i2d(\beta - \kappa)} [(e^{i2dN\kappa} - 1) + N\delta_{n,m}]. \quad (31)$$

We use this expression to calculate numerical values for S_{nm} to be used in our simulations later.

The other blocks of the Jacobi matrix are

$$J_{n>0} = \begin{pmatrix} e^{-i2dN\kappa} & 0 & R \\ 0 & e^{i2dN\kappa} & R \\ -2\epsilon(1-r)R & -2\epsilon(1-r)R & 1 - \epsilon(1 + 2rR^2) \end{pmatrix}.$$

The eigenvalues may be written down explicitly as roots of the associated cubic polynomials.

Two conclusions are apparent in the all-to-all coupled case. First, since the propagation constant β cancels out of the expression for the Jacobi matrix, the stability of the in-phase state does not depend on the particular properties of

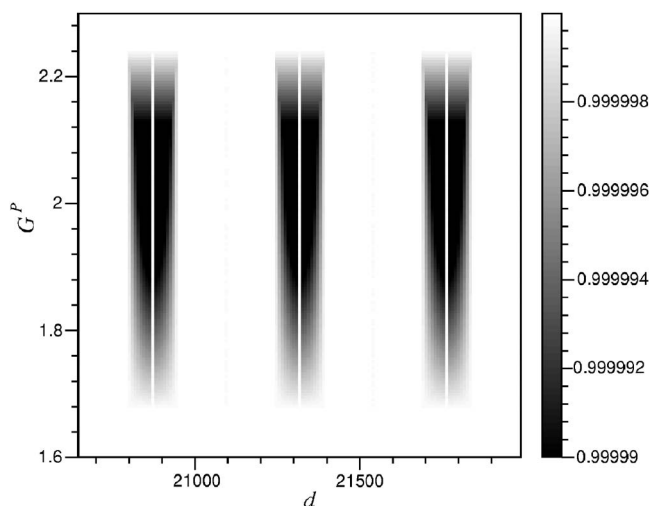


FIG. 3. Contour plot of the leading stability eigenvalue for the in-phase solution in the all-to-all coupling case. The coupling coefficient is $\kappa=0.001 \mu\text{m}^{-1}$ and the field reflection from the output face is $r=0.187$.

the individual fiber lasers. Second, since the matrix J_n depends on coupling parameters N, d , and κ only through the combination $e^{\pm i2dN\kappa}$ the stability eigenvalues change periodically as any of these parameters is increased.

According to our calculations the stability of the in-phase solution depends sensitively on the coupler geometry. The coupling coefficient κ enters the expressions for the eigenvalues merely as a length scale. The periodic dependence of the eigenvalues on the product $dN\kappa$ translates into periodic regions of stability for the inphase state. An example is shown in Fig. 3 where the magnitude of the leading eigenvalue is plotted over a range of coupler lengths d . As expected, the stability islands occur periodically, in pairs, around parameter values specified by condition $dN\kappa=(m+1/2)\pi$, where $m=0,1,2,\dots$. For the example drawn in Fig. 3 we used propagation constant $\beta=8 \mu\text{m}^{-1}$, and coupling constant $\kappa=0.001 \mu\text{m}^{-1}$, parameter values that are typical for optical waveguide couplers. We see that for a coupler of length $d=20\,870 \mu\text{m}$ there is a stable coherent solution over a range of pumping parameters.

Simulations of the full nonlinear system were used to further investigate stability. Calculating the basin of attraction for this type of multidimensional system is computationally intensive. Even given this basin it is challenging to represent the resulting $3N$ -dimensional body in a satisfactory way. Instead we evaluated the size of the basin by picking an ensemble of initial conditions which were random perturbations of the in-phase solution and in each case iterating the map to see whether the system relaxed to the in-phase state. The results indicate that the basin of attraction is relatively small, of order 10^{-2} in terms of units $\sqrt{I_{\text{sat}}}$. It is therefore unlikely that the in-phase solution would be robust enough to be of practical use, unless one is able to fabricate and control the system to a fine tolerance. Furthermore, with such a small basin, the attractor might be especially sensitive to dynamical noise.

Simulations were also used to investigate the system for pump levels beyond the onset of the Hopf threshold Eq. (10),

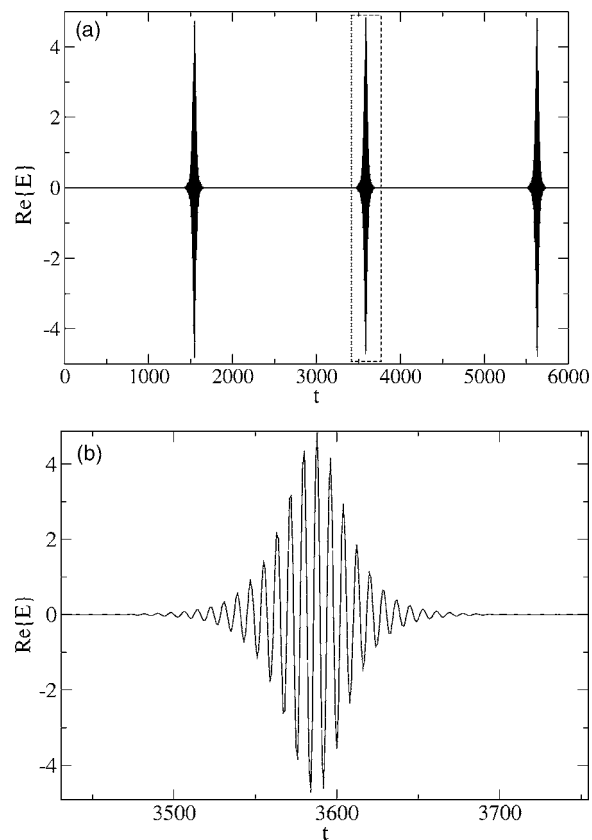


FIG. 4. An array of seven equally pumped ($G^P=2.3$) lasers in an in-phase pulsing state. Shown in (a) are the real components of the electric fields over 6000 round trips. Panel (b) plots one of these pulsing events by magnifying the dashed box in panel (a). Results for all seven fibers coincide in the diagram.

keeping the other parameters fixed. In agreement with the single fiber case, the intensity and gain become time dependent. While the temporal dependence can be complicated, as shown in Fig. 4, we find a stable in-phase attractor is created. However, the basin of attraction of this in-phase state is again relatively small.

Let us summarize the key results of this section for all-to-all coupling of identical fiber elements. First, the stability of the in-phase state is independent of the individual fiber properties. Second, the stability eigenvalues are strictly periodic functions of the product $2dN\kappa$ so that for a fixed number of fibers and a fixed coupling parameter κ , stability islands occur periodically as a function of coupler length. Third, the in-phase attractor has a relatively small basin of attraction. These properties appear to persist beyond the threshold for pulsing.

V. NEAREST NEIGHBOR COUPLING

For nearest neighbor coupling of fibers arranged in a ring (see Fig. 5), the coupling generator matrix M can be written as $M_{kl}=\beta\delta_{k,l}+\kappa\delta_{k,l+1}+\kappa\delta_{k,l-1}$, with $k,l=0,1,\dots,N-1$, and taking the indices k,l modulo N is implied. The eigenvalues of the coupling matrix can be found by diagonalizing S ,

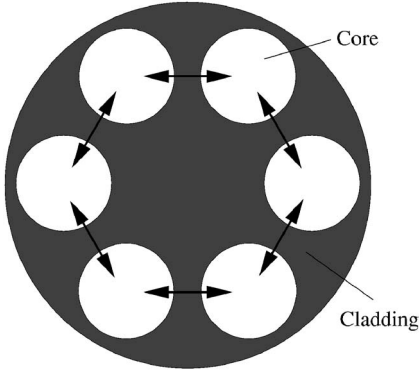


FIG. 5. Ring coupler cross section with identical fibers.

$$(U^* S U)_{nm} = (e^{iU^* M U})_{nm} = e^{i2d[\beta + 2\kappa \cos(2\pi n/N)]} \delta_{nm}. \quad (32)$$

Once again, S is circulant so that the full reduction to Eq. (27) is possible. From the expression above we find that there are degenerate eigenvalues $\lambda_k = \lambda_{N-k}$. The in-phase state is nondegenerate, and its frequency ω is obtained from λ_0 with result

$$\omega = -2d(\beta + 2\kappa). \quad (33)$$

To express S in terms of the parameters β and κ we apply the inverse transformation to obtain

$$S_{nm} = [U(U^* S U)U^*]_{nm} = \frac{1}{N} \sum_{k=0}^{N-1} e^{i2\pi(n-m)k/N} e^{i2d[\beta + 2\kappa \cos(2\pi k/N)]}, \quad (34)$$

which will be useful later in the analysis. The linearized equations for the system can then be block diagonalized using the transformation U . The Jacobi matrix for the system consists of N blocks:

$$J_{n>0} = \begin{pmatrix} e^{i4d\kappa[\cos(2\pi n/N)-1]} & 0 & R \\ 0 & e^{-i4d\kappa[\cos(2\pi n/N)-1]} & R \\ -2\epsilon(1-r)R & -2\epsilon(1-r)R & 1 - \epsilon(1+2rR^2) \end{pmatrix}. \quad (35)$$

This is similar to the result for the all-to-all coupled case, but with one important difference. Consider for example a ring of six fibers. Repeating the same calculations as for the all-to-all case we find that blocks $J_{n>0}$ have stable eigenvalues provided that phases of the main diagonal elements $e^{\pm i4d\kappa[\cos(2\pi n/N)-1]}$ are nearly odd multiples of π . This condition is satisfied simultaneously for blocks $J_1, J_2, J_4,$ and J_5 when $d\kappa \approx (m+1/2)\pi$, with $m=0, 1, 2, \dots$. But, at the same time the phases of the main diagonal elements of block J_3 are *even* multiples of π . So, when other blocks satisfy the stability condition, block J_3 does not. It follows that in the case of six fibers the ring configuration with nearest neighbor coupling never yields a stable in-phase solution, regardless of the individual fiber properties.

More generally, for any even-number ring array blocks J_0 and $J_{N/2}$ will have stable eigenvalues at opposite intervals in

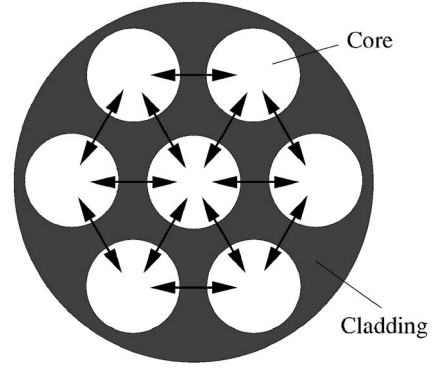


FIG. 6. Star coupler cross section with identical fibers.

the parameter space with respect to the coupler length d . Therefore the in-phase state solution is unstable for all even numbered ring configurations. In case of odd-number ring arrays, different Jacobi matrix blocks J_n will yield stable eigenvalues at incommensurate intervals with respect to d . Although it is generally possible to find a coupler length at which all blocks yield stable eigenvalues, the stability regions are relatively rare and occur less frequently as the number of fibers N is increased. Stability of such a system is at best the same as for the all-to-all coupled case.

VI. STAR CONFIGURATION

In this configuration there are N fibers on a ring and another fiber going through the middle (see Fig. 6). We label the middle fiber with the index N , and those around it with $k=0, 1, 2, \dots, N-1$. We consider nearest neighbor coupling.

The first observation is that in general there is no (fully symmetric) in-phase state when all the fibers are equally pumped. This directly reflects the lower symmetry of the star configuration: the central fiber (with N neighbors) is manifestly different than those on the ring (with three neighbors). In order that an in-phase state exist, we must either consider uneven pumping of the laser elements or specially design (or tune) the coupling matrix parameters. In the latter strategy, the existence of an in-phase solution is equivalent to the requirement that S has an in-phase eigenvector, that is $\mathbf{S}\mathbf{y}^{(0)} = \lambda_0 \mathbf{y}^{(0)}$, where $\mathbf{y}^{(0)} = (1, 1, \dots, 1)^T$. In some sense, we can view these parameter-tuning strategies as introducing an accidental symmetry. That is, we spoiled the symmetry of the pure ring by adding a nonequivalent central fiber, but then restore the in-phase state by tuning the parameters.

The generator matrix for this configuration can be written as

$$M_{kl} = \beta \delta_{k,l} + \kappa (\delta_{k,l+1} + \delta_{k,l-1}) + \beta_N \delta_{k,N} \delta_{N,l} + \kappa_N (\delta_{N,l} + \delta_{k,N}), \quad (36)$$

where $k, l < N$. We now derive a simple condition on the coupling parameters which guarantees the existence of the desired in-phase state, by demanding that $S = e^{i2dM}$ has an inphase eigenvector.

From the symmetry of the coupler we see that the elements of the coupling matrix S will satisfy $S_{Nk} = S_{kN} = S_{lN}$.

Although S is no longer circulant, a submatrix is, i.e., the elements S_{kl} for $k, l=0, \dots, N-1$. From the form of S we can explicitly determine its elements in terms of the parameters appearing in M , using the procedure used in each of the previous cases, i.e., the transformations indicated by Eqs. (31) and (34). After some algebra we find

$$a = S_{NN} = e^{id(\beta+\beta_N+2\kappa)} \left[\cos(d\sqrt{D}) - i \frac{\beta - \beta_N + 2\kappa}{\sqrt{D}} \sin(d\sqrt{D}) \right], \quad (37)$$

$$b = S_{N0} = e^{i2d(\beta+\beta_N+2\kappa)} (-i) \frac{2\kappa_N}{\sqrt{D}} \sin(d\sqrt{D}), \quad (38)$$

and the sum

$$\sigma = \sum_{k=0}^{N-1} S_{0k} = e^{id(\beta+\beta_N+2\kappa)} \times \left[\cos(d\sqrt{D}) + i \frac{\beta - \beta_N + 2\kappa}{\sqrt{D}} \sin(d\sqrt{D}) \right], \quad (39)$$

where $D = (\beta - \beta_N + 2\kappa)^2 + 4N\kappa_N^2$.

Let us look first at the case of a lossless coupler, where $\beta^i = 0$ and $\beta_N^i = 0$. To keep our presentation simple we shall consider coupling on a triangular lattice where $N=6$, and also assume that $\beta_N^r = \beta^r$, and $\kappa_N = \kappa$ is real. (Our calculations for more general cases yielded qualitatively similar results.) For these parameter values it follows from the expressions above that for a coupler length

$$d_m = \frac{m\pi}{2\sqrt{7}\kappa}, \quad m = 0, 1, 2, \dots \quad (40)$$

the quantity b is zero, so that the center fiber is virtually decoupled from the others, and

$$a = \sigma = (-1)^m e^{i2d(\beta+\kappa)}. \quad (41)$$

Therefore the in-phase eigenvector exists for coupler lengths given by Eq. (40) and its eigenvalue is $\lambda_0 = \sigma$.

Turning to the stability of the in-phase solution consider the eigenvalues of the Jacobi matrix. We can block diagonalize that matrix by applying the coordinate transformation Eq. (15) to the linearized equations, and then eliminate any explicit time dependence via transformation Eq. (26). In the new coordinates the linearized equations become

$$u'_n = (\lambda_n/\lambda_0)u_n + Rg_n, \quad (42)$$

$$v'_n = (\lambda_n/\lambda_0)^* v_n + Rg_n, \quad (43)$$

$$g'_n = g_n - \epsilon(1 + 2rR^2)g_n - 2\epsilon(1-r)R(u_n + v_n), \quad (44)$$

$$u'_N = u_N + Rg_N, \quad (45)$$

$$v'_N = v_N + Rg_N, \quad (46)$$

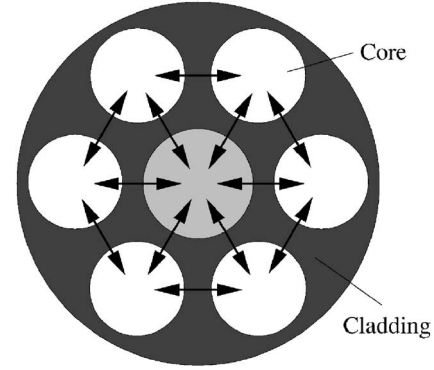


FIG. 7. Star coupler cross section with nonidentical fibers.

$$g'_N = g_N - \epsilon(1 + 2rR^2)g_N - 2\epsilon(1-r)R(u_N + v_N), \quad (47)$$

where the λ_n are eigenvalues of the circulant submatrix of S . As with the nearest neighbors on a ring, we obtain $N+1$ blocks of size 3×3 . Blocks J_0 and J_N are the same as the single fiber Jacobian evaluated at its fixed point Eq. (8):

$$J_0 = J_N = \begin{pmatrix} 1 & 0 & R \\ 0 & 1 & R \\ -2\epsilon(1-r)R & -2\epsilon(1-r)R & 1 - \epsilon(1 + 2rR^2) \end{pmatrix},$$

while the other blocks have the same form as Eq. (35):

$$J_{n>0} = \begin{pmatrix} (\lambda_n/\lambda_0) & 0 & R \\ 0 & (\lambda_n/\lambda_0)^* & R \\ -2\epsilon(1-r)R & -2\epsilon(1-r)R & 1 - \epsilon(1 + 2rR^2) \end{pmatrix}.$$

This result makes sense as the outside fibers are effectively decoupled from the center fiber. The difference is that we now have two blocks that have a unity eigenvalue for all parameter values, so that even if all the other eigenvalues lie inside the unit circle, the in-phase state is neutrally stable to linear order. This means that stability is determined by higher order terms, so that any attraction to the in-phase state will be weak.

We summarize our main results for the star configuration. First, the lower symmetry of this configuration implies that in the case of identical elements there is no in-phase state. However, we observe that introducing nonuniformity either in the coupling parameters or the individual fibers can yield an in-phase state. In the case of a lossless coupler an in-phase state will be stable provided the coupler length is specially tuned. This in-phase state is, at best, weakly stable.

VII. ROBUST COHERENT SYNCHRONIZATION WITH THE STAR CONFIGURATION

The results of the previous calculations suggest a strategy for designing a robustly phase coherent fiber array. The neutral linear stability of the star configuration implies that small modifications of the basic design can have a substantial effect on the dynamics of the array. In this section, we present a modification of the star configuration that results in well-ordered phase coherence that is stable and attracting (see Fig. 7).

To this end, we include small losses in the coupler, introducing loss parameters $\delta_N = 2d_m\beta_N^i$ for the central fiber and $\delta = 2d_m\beta^i$ for the outer fibers. We assume these two parameters are small (so $\delta, \delta_N \ll 1$) but of the same order (so $\delta \sim \delta_N$). We will show that these can be chosen in a way that admits a solution very similar to the in-phase solution in the lossless case but with improved stability properties.

The first observation is that no strictly in-phase solution exists for the generic case $\delta \neq \delta_N$ no matter how small the difference [cf. Eqs. (A12) and (A13)]. However, if the pump of the central fiber is turned off, there exists a state where all six outside fibers are synchronized in phase, while the field in the center fiber is phase shifted but $O(\delta)$ smaller in amplitude: $\tilde{E}_n = Re^{-i\omega t}$, $\tilde{G}_n = \ln(1/\varrho)$, and $\tilde{E}_N = Re^{-i\omega t} y_N^{(0)}$, $\tilde{G}_N = 0$, where ϱ is the total loss in the system over one round trip time, and $e^{-i\omega}$ is the eigenvalue of the round trip operator A . Explicit expressions for $y_N^{(0)}$ and ω are derived in the Appendix. Since the dissipation in the fibers is small, we can expand all expressions to leading order in δ and δ_N . Then the field amplitudes $|E_n|$ for the fibers in the ring are obtained from Eq. (2) as

$$|E_n|^2 = R^2 = \frac{G^P - \ln(1/\varrho)}{2(1 - \varrho)}, \quad (48)$$

where

$$\varrho = r\alpha = r \left(1 - \frac{4\delta + 3\delta_N}{7} \right) + O(\delta^2), \quad (49)$$

and the parameter α describes the loss in the coupler. The field amplitude in the center fiber is

$$|E_N| = |R y_N^{(0)}| = \frac{3rR}{7(1 - r)} (\delta - \delta_N) + O(\delta^2) \quad (50)$$

and it gives only a minor contribution to the interference pattern at the output of the array.

Since the central fiber field is $O(\delta)$ smaller than that in the outer fibers, this solution produces virtually the same far field image as the in-phase state of the ring configuration for the same pumping power. To demonstrate its stability properties, we turn to the linearized problem. Noting that $G_N = 0$, Eq. (11) can be block diagonalized by applying the Fourier transformation Eq. (15) to the circulant part of the system ($n < N$), with the result

$$\psi'_n = \frac{b}{\alpha} \sqrt{N} \psi_N \delta_{0,n} + \frac{\lambda_n}{\alpha} \psi_n + \frac{1}{\alpha} (b\tilde{E}_N + \sigma\tilde{E}_n) g_n, \quad (51)$$

$$\chi'_n = \frac{b^*}{\alpha} \sqrt{N} \chi_N \delta_{0,n} + \frac{\lambda_n^*}{\alpha} \chi_n + \frac{1}{\alpha} (b\tilde{E}_N + \sigma\tilde{E}_n)^* g_n, \quad (52)$$

$$g'_n = -2\epsilon(1 - \alpha r) \tilde{E}_n^* \psi_n - 2\epsilon(1 - \alpha r) \tilde{E}_n \chi_n + [1 - \epsilon(1 + 2r\alpha|\tilde{E}_n|^2)] g_n, \quad (53)$$

$$\psi'_N = r\alpha\psi_N + r\sqrt{N}b\psi_0 + r(a\tilde{E}_N + Nb\tilde{E}_n) g_N, \quad (54)$$

$$\chi'_N = r\alpha^* \chi_N + r\sqrt{N}b^* \chi_0 + r(a\tilde{E}_N + Nb\tilde{E}_n)^* g_N, \quad (55)$$

$$g'_N = [1 - \epsilon(1 + 2\alpha|\tilde{E}_N|^2)] g_N. \quad (56)$$

After substituting values for \tilde{E}_N and \tilde{E}_n , and getting rid of the explicit time dependence by transformation Eq. (26) the linearized equations become

$$u'_n = (b/\nu) \sqrt{N} \delta_{n,0} + (\lambda_n/\nu) u_n + R g_n, \quad (57)$$

$$v'_n = (b/\nu)^* \sqrt{N} \delta_{n,0} + (\lambda_n/\nu)^* v_n + R g_n, \quad (58)$$

$$g'_n = -2\epsilon(1 - \rho) R u_n - 2\epsilon(1 - \rho) R v_n + [1 - \epsilon(1 + 2\rho R^2)] g_n, \quad (59)$$

$$u'_N = \rho(a/\nu) u_N + \rho \sqrt{N} (b/\nu) u_0 + y_N^{(0)} R, \quad (60)$$

$$v'_N = \rho(a/\nu)^* v_N + \rho \sqrt{N} (b/\nu)^* v_0 + y_N^{(0)*} R, \quad (61)$$

$$g'_N = [1 - \epsilon(1 + 2|y_N^{(0)}|^2 R^2)] g_N, \quad (62)$$

where λ_0 is the in-phase eigenvalue for the circulant submatrix of the coupling matrix S and $\nu = \alpha e^{-i\omega}$; to leading order these are

$$\lambda_0 = \sigma = (-1)^m e^{i2d_m(\beta^r + \kappa)} \left(1 - \frac{4\delta + 3\delta_N}{7} \right) + O(\delta^2), \quad (63)$$

and $\nu = \sigma + O(\delta^2)$.

The Jacobi matrix can be represented in block diagonal form with one 6×6 block and five 3×3 blocks. Note that the propagation constants β^r cancel out from the expressions for the Jacobi matrix through order δ as long as all of the fibers have the same propagation constant. Thus, just as in the previous cases, the coupling parameter κ enters the stability problem solely as a length scale. Since we are considering couplers with a specific length, the coupling parameter itself cancels out of the expression for the Jacobi matrix.

The 3×3 blocks of the Jacobi matrix can be written as

$$J_{n>0} = \begin{pmatrix} (\lambda_n/\nu) & 0 & R \\ 0 & (\lambda_n/\nu)^* & R \\ -2\epsilon(1 - \rho)R & -2\epsilon(1 - \rho)R & 1 - \epsilon(1 + 2\rho R^2) \end{pmatrix},$$

where

$$\lambda_n/\nu = (-1)^m e^{i(m\pi/\sqrt{7})[2 \cos(2\pi n/N) - 1]} \left(1 - 3 \frac{\delta - \delta_N}{7} \right) + O(\delta^2). \quad (64)$$

If the other small parameter in the system ϵ is of the same order or smaller than the loss in the coupler $\epsilon \leq \delta$, then to $O(\delta)$ the stability eigenvalues depend on the loss in the coupler only through the difference $\delta - \delta_N$. Numerical calculations for stability eigenvalues suggest that for the value of $\epsilon \sim 10^{-4}$, which is characteristic for fiber laser systems, a simple synchronization condition holds over a range of values for δ and δ_N (Fig. 8):

$$\delta > \delta_N. \quad (65)$$

Thus the state is stable provided the coupler loss parameter of the center fiber is smaller than that of the outer fibers.

The remaining 6×6 block of the Jacobi matrix is, to $O(\delta)$,

$$J_0 = \begin{pmatrix} 1 & 0 & R & \sqrt{N}(b/\nu) & 0 & 0 \\ 0 & 1 & R & 0 & \sqrt{N}(b/\nu)^* & 0 \\ -2\epsilon(1-\varrho)R & -2\epsilon(1-\varrho)R & 1-\epsilon(1+2\varrho R^2) & 0 & 0 & 0 \\ \varrho\sqrt{N}(b/\nu) & 0 & 0 & \varrho(a/\nu) & 0 & y_N^{(0)}R \\ 0 & \varrho\sqrt{N}(b/\nu)^* & 0 & 0 & \varrho(a/\nu)^* & y_N^{*(0)}R \\ 0 & 0 & 0 & 0 & 0 & 1-\epsilon \end{pmatrix},$$

where

$$a/\nu = 1 + \frac{\delta - \delta_N}{7} + O(\delta^2) \quad (66)$$

and

$$b/\nu = -\frac{\delta - \delta_N}{14} + O(\delta^2). \quad (67)$$

The upper left 3×3 block of J_0 has the same form as the single fiber Jacobian. The lower right 3×3 block is an upper triangular matrix, which has elements on its main diagonal with magnitudes all smaller than 1. The two blocks are coupled through terms proportional to b/ν which are themselves $O(\delta)$ and therefore small. Therefore the leading eigenvalue of J_0 behaves similarly to the leading eigenvalue of the single fiber laser. Just as in the all-to-all coupled case, it is the leading eigenvalue of J_0 that governs the onset of lasing and the onset of pulsing (Fig. 9).

To this point, we have shown that the ‘‘nearly in-phase’’ state is stable within the pumping range $G_{tc}^P < G^P < G_h^P$ as long as $\delta > \delta_N$. Our calculations assumed the particular cou-

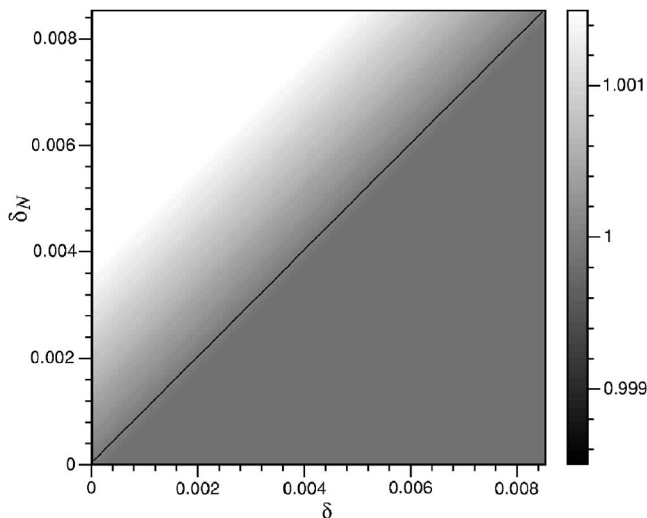


FIG. 8. Contour plot of the leading stability eigenvalue for the coherent state for the star coupler.

pler length given by Eq. (40). To examine this state beyond the analytically tractable regime, we once again turn to numerical simulations.

As a figure of merit for the coherence of the array output, we introduce a synchronization parameter

$$s = \left\langle \frac{\left| \sum_i E_i \right|}{\sum_i |E_i|} \right\rangle_t. \quad (68)$$

Here index i denotes the i th fiber in the array and $\langle \cdot \rangle_t$ denotes a time average. This quantity takes on its maximum value of unity when all fibers are synchronized in-phase and has a near zero value for incoherent arrays. The contribution of each field to the synchronization parameter is weighted by the magnitude of that field. In the special case when all the magnitudes are the same and the phases are uniformly distributed, s is zero. The parameters we used in our simulations are $\beta^r = \beta_N^r = 8 \mu\text{m}^{-1}$, $\beta_N^i = 0.8 \times 10^{-7} \mu\text{m}^{-1}$, $\beta^i = 2 \times 10^{-7} \mu\text{m}^{-1}$, $\kappa_N = \kappa = 0.001 \mu\text{m}^{-1}$. The coupler length is $d \sim 2$ cm. As a check, the simulations agree with our analytical results: stable coherent solutions are found for coupler lengths Eq. (40), with the predicted frequency and amplitude (Fig. 10). Our numerical investigations show that these solutions are globally attracting for typical conditions—the system spontaneously synchronizes to the in-phase state. The system is also robust with respect to changes in the system parameters.

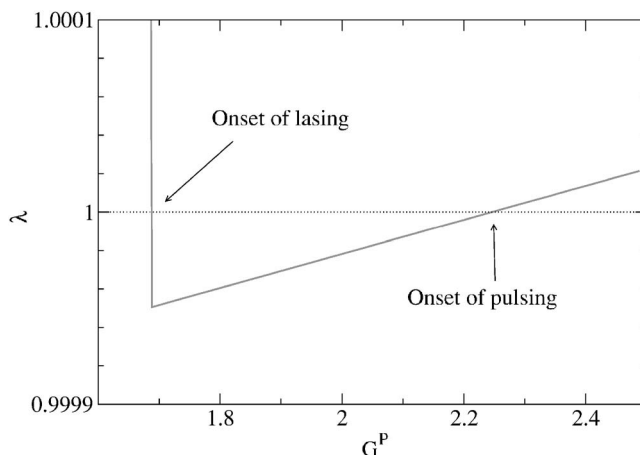


FIG. 9. Leading eigenvalue of J_0 block vs pump.

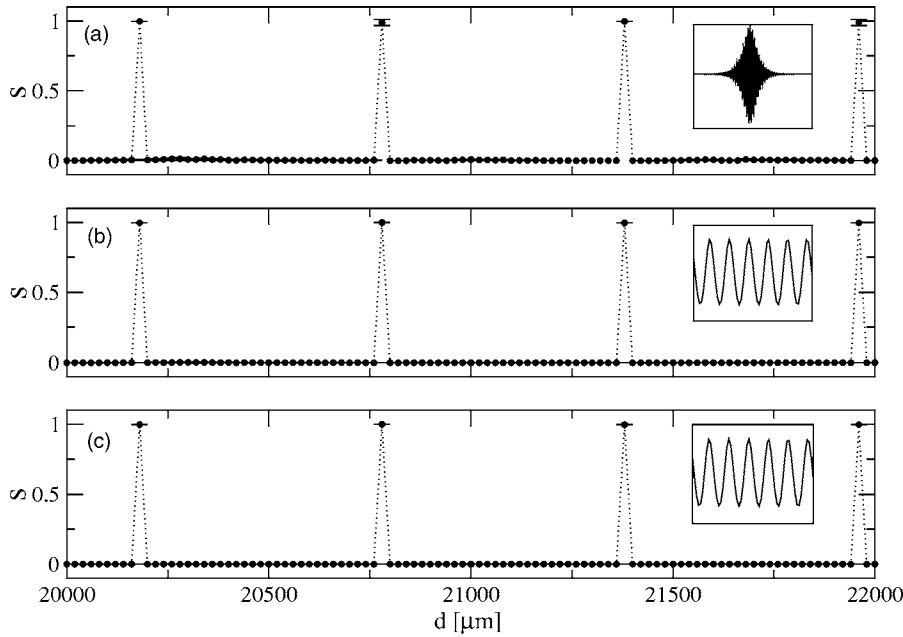


FIG. 10. Synchronization parameter plotted against length of the coupler. The system synchronizes for coupler lengths given by Eq. (40). The pumping parameter is (a) $G^p=2.5$, (b) $G^p=2.1$, and (c) $G^p=1.8$. Insets show typical time series for the in-phase solution at that pump level. The synchronization properties of the system seem not to change with pump level, even as the output changes from simple periodic (c) to pulsing (a).

The most critical parameter is the length of the coupler insofar as our analytic results guarantee stability for specific coupler lengths Eq. (40). Our simulations demonstrate that these synchronous solutions persist for a rather sizable 20- μm range around these characteristic lengths.

To push still further beyond the analytically tractable regime, we ran numerical simulations to see what happens to the coherent synchronized state above the pulsing threshold. We find that coherence is maintained. Even though our stability analysis was restricted to constant gain states, it appears that similar (or possibly even the same) conditions hold for stable coherent pulsing solutions. If we zoom in on the regions of stability, as in Fig. 11, we see that the stability of the in-phase solution is robust with respect to changes in array length. The region of stability is $\sim 20 \mu\text{m}$ wide, and

does not change as the pumping is increased. We also investigated numerically what happens if there are imperfections in the coupler. Our results suggest that the globally stable coherent solution persists if we add small but finite perturbations to the elements of coupling matrix S .

Since the coherent solution appears to be globally stable and robust with respect to small changes in system parameters, it is reasonable to expect it to persist even in models that include noise.

VIII. SUMMARY

We have carried out a stability analysis of a recently proposed laser array model [10]. Our main motivation was to provide insight into how to generate stable, highly ordered

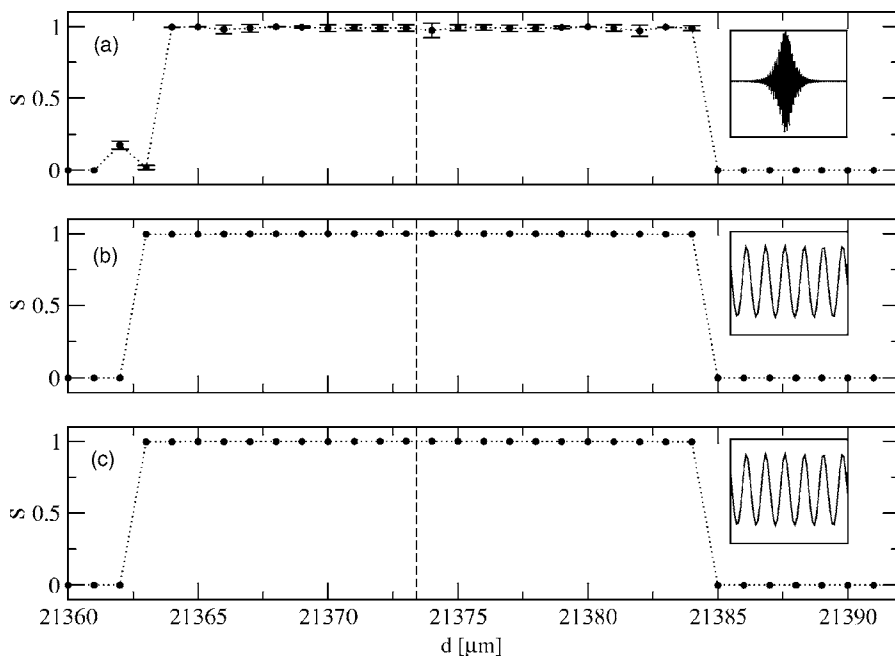


FIG. 11. The width of the stability region for the coherent state is finite, and does not appear to depend on pumping level. The dashed line denotes the analytically predicted optimal length of the coupler Eq. (40). Pumping parameter is set to (a) $G^p=2.5$, (b) $G^p=2.1$, and (c) $G^p=1.8$. Insets show typical time series for the in-phase solution at that pump level.

dynamical states. The role of symmetry is expected to be important in the formation of such states [8,9]. Four cases were considered with varying degrees of symmetry; the limiting case of all-to-all (global) coupling and then three locally connected cases. In the all-to-all coupled example we found regions of stable in-phase solutions though with rather small basins of attraction. In contrast, in the locally connected ring configuration the in-phase solution was unstable. Including a seventh element in the ring center (star configuration) that is equally coupled to all the ring elements at best renders the in-phase state only weakly stable (i.e., linearly neutrally stable). In the fourth and last configuration, by introducing small losses and simultaneously lowering the system's symmetry—with unequal coupler losses and by underpumping center fiber—the system displays a broadly stable, phase coherent synchronized state which is attracting for typical initial conditions.

The synchronization condition (65) for this last configuration is worth considering a bit further. The synchronous solution is globally attracting only if the loss within the coupler is smaller in the center fiber than in the other fibers. This is somewhat counterintuitive insofar as the center fiber is underpumped, so that the overall dissipation in it is much larger than any of the losses incurred within the coupler.

Although configurations of six fibers on the ring, and seven fibers with the middle one underpumped, are apparently similar, they behave quite differently. Therefore the underpumped fiber must play a crucial role in array synchronization even though its field is small and does not contribute significantly to the total output from the array. This is qualitatively similar to the behavior observed in experiments [14], where the best synchronization is achieved when some of the fibers in the array were underpumped. It is tempting to speculate that there may be an underlying mechanism for the array synchronization, which requires a certain number of fibers in the array to be passive [35].

Fiber lasers are known to be inherently noisy systems, and further refinements of model (1) and (2) in that direction is warranted. We anticipate that the presence of noise would wipe out weakly stable coexisting solutions such as the ones described in Sec. IV. On the other hand, we expect the globally stable solutions obtained by symmetry breaking to persist.

An important aspect of real fiber arrays is the highly multimode nature of the individual lasers. The model we have analyzed describes a single longitudinal mode, and it remains to be seen whether it can capture the essential features seen in experiments using fiber arrays, although preliminary indications are promising. It has been suggested [36] that the presence of many longitudinal modes can be handled by purely statistical means since mode-mode interactions are typically weak [27]. In that case, a hybrid description may be a fruitful approach, with the synchronization dynamics governed by a model like the present one, which captures the strong interactions between matched longitudinal modes in different fibers, and the multimode aspects governed by the statistical superposition of weakly interacting sets of these mode groups. Such a hybrid scheme can be very successful in studying complex nonlinear dynamical systems, as has been demonstrated for example in the study of two dimen-

sional arrays of superconducting Josephson junctions [37,38].

ACKNOWLEDGMENTS

The idea that turning off the power to one or more fibers can improve the overall coherence of an array is due to Monica Minden. This work was supported in part by ONR Grant No. N00014-99-1-0592 and HRL Laboratories Grant No. SR04.2172. S.P. and K.W. thank Denis Tsygankov for helpful discussions.

APPENDIX

In the general case the coupling matrix for the star coupler described in Sec. VI has the form

$$S = \begin{pmatrix} c_0 & c_1 & \dots & c_{N-2} & c_{N-1} & b \\ c_{N-1} & c_0 & \dots & c_{N-3} & c_{N-2} & b \\ \vdots & & \ddots & & \vdots & \vdots \\ c_2 & c_3 & \dots & c_0 & c_1 & b \\ c_1 & c_2 & \dots & c_{N-1} & c_0 & b \\ b & b & \dots & b & b & a \end{pmatrix}.$$

Elements c_k make up a circulant [33] submatrix within S . The eigenvalue equations for S can be written as

$$by_N + \sum_{k=0}^{m-1} c_{N-m+k} y_k + \sum_{k=m}^{N-1} c_{k-m} y_k = \lambda y_m, \quad m \neq N, \quad (\text{A1})$$

$$ay_N + b \sum_{k=0}^{N-1} y_k = \lambda y_N. \quad (\text{A2})$$

After substituting new dummy summation index $p=N-m+k$ in the first sum, and $l=k-m$ in the second sum in Eq. (A1), the eigenvalue equations assume the form

$$by_N + \sum_{p=N-m}^{N-1} c_p y_{p+m-N} + \sum_{l=0}^{N-m-1} c_l y_{l+m} = \lambda y_m, \quad (\text{A3})$$

$$ay_N + b \sum_{k=0}^{N-1} y_k = \lambda y_N \quad (\text{A4})$$

or more conveniently written, changing back to k as a summation index,

$$by_N + \sum_{k=0}^{N-m-1} c_k y_{k+m} + \sum_{k=N-m}^{N-1} c_k y_{k+m-N} = \lambda y_m, \quad (\text{A5})$$

$$ay_N + b \sum_{k=0}^{N-1} y_k = \lambda y_N. \quad (\text{A6})$$

If we assume that the solution to these equations can be found in the form $y_k = \rho^k$, for $k \neq N$, we can write

$$by_N + \sum_{k=0}^{N-m-1} c_k \rho^{k+m} + \rho^{-N} \sum_{k=N-m}^{N-1} c_k \rho^{k+m} = \lambda \rho^m, \quad (\text{A7})$$

$$ay_N + b \sum_{k=0}^{N-1} \rho^k = \lambda y_N. \quad (\text{A8})$$

Further assuming that $\rho^{-N}=1$ we obtain the following expressions:

$$by_N/\rho^m + \sum_{k=0}^{N-m-1} c_k \rho^k + \sum_{k=N-m}^{N-1} c_k \rho^k = \lambda, \quad (\text{A9})$$

$$ay_N + b \sum_{k=0}^{N-1} \rho^k = \lambda y_N, \quad (\text{A10})$$

where ρ must be a root of the equation $\rho^{-N}=1$, and therefore can assume values $\rho_m = e^{-i2\pi m/N}$, with $m=0, 1, \dots, N-1$. For $m \neq 0$ the system above has a solution only if $y_N=0$. The eigenvalues are then given by

$$\lambda_m = \sum_{k=0}^{N-1} c_k e^{-i2\pi m k/N}, \quad m \neq 0, N \quad (\text{A11})$$

with corresponding eigenvectors $\mathbf{y}^{(m)} = (1, e^{-i2\pi m/N}, e^{-i4\pi m/N}, \dots, e^{-i2\pi(N-1)m/N}, 0)^T$, where T denotes the transpose. These eigenvalues coincide with the eigenvalues for the circular submatrix of S .

For $m=0$ the eigenvalue equations are

$$by_N + \sum_{k=0}^{N-1} c_k = \lambda, \quad (\text{A12})$$

$$ay_N + bN = \lambda y_N. \quad (\text{A13})$$

By solving these equations for y_N and λ one finds

$$\lambda_{0,N} = \frac{a+\sigma}{2} \pm \sqrt{\left(\frac{\sigma-a}{2}\right)^2 + Nb^2} \quad (\text{A14})$$

and corresponding eigenvectors

$$\mathbf{y}^{(0),(N)} = \left[1, 1, \dots, 1, \frac{a-\sigma}{2b} \pm \sqrt{\left(\frac{\sigma-a}{2b}\right)^2 + N} \right]^T. \quad (\text{A15})$$

For constant gain solutions the round trip operator A is constant in time, and therefore the solutions to the map Eqs.

(1) and (2) have to be eigenvectors of A . In order to find these solutions, we carry out a similar eigensystem calculation for the roundtrip operator as we did for the coupling matrix S . For the lossy coupler with pumping for the center fiber turned off, as described in Sec. VII, the round trip operator has the form

$$A = \frac{1}{\alpha} \begin{pmatrix} c_0 & c_1 & \dots & c_{N-2} & c_{N-1} & b \\ c_{N-1} & c_0 & \dots & c_{N-3} & c_{N-2} & b \\ \vdots & & \ddots & & \vdots & \vdots \\ c_2 & c_3 & \dots & c_0 & c_1 & b \\ c_1 & c_2 & \dots & c_{N-1} & c_0 & b \\ \varrho b & \varrho b & \dots & \varrho b & \varrho b & \varrho a \end{pmatrix},$$

where $\varrho = r\alpha$, and $\alpha < 1$ is the coupler loss parameter. First, we find the eigensystem for the matrix αA by retracing the steps in the analysis for S . We find that $N-1$ eigenvalues are the same,

$$\lambda_m = \frac{1}{\alpha} \sum_{k=0}^{N-1} c_k e^{-i2\pi m k/N}, \quad m \neq 0, N \quad (\text{A16})$$

as well as their associated eigenvectors $\mathbf{y}^{(m)} = (1, e^{-i2\pi m/N}, e^{-i4\pi m/N}, \dots, e^{-i2\pi(N-1)m/N}, 0)^T$. The other two eigenvalues are given by

$$\nu_{\pm} = \frac{\varrho a + \sigma}{2} \pm \sqrt{\left(\frac{\sigma - \varrho a}{2}\right)^2 + \varrho N b^2} \quad (\text{A17})$$

and their corresponding eigenvectors are

$$\mathbf{y}^{(0),(N)} = \left[1, 1, \dots, 1, \frac{\varrho a - \sigma}{2b} \pm \sqrt{\left(\frac{\sigma - \varrho a}{2b}\right)^2 + \varrho N} \right]^T. \quad (\text{A18})$$

These are coherent solutions to the system Eqs. (1) and (2). The eigenvalues for the roundtrip operator are then simply ν_{\pm}/α . A coherent solution is a steady state (periodic) solution if its eigenvalues lie on the unit circle, i.e., if the transcendental equation $|\nu(\alpha)| = \alpha$ has a solution. That means that the gain is equal to the loss for the Eq. (A18) eigenmode. What is left to do is to check if such a solution is stable. The linear stability analysis is carried out in Sec. VII.

[1] S. H. Strogatz, *SYNC: The Emerging Science of Spontaneous Order* (Hyperion, New York, 2003).
 [2] A. Pikovsky, M. Rosenblum, and J. Kurths, *Synchronization: A Universal Concept in Nonlinear Science* (Cambridge University Press, Cambridge, England, 2001).
 [3] R. A. York, IEEE Trans. Microwave Theory Tech. **41**, 1799 (1993).
 [4] P. Liao and R. A. York, IEEE Trans. Microwave Theory Tech. **41**, 1810 (1993).
 [5] T. Heath, R. Kerr, and G. Hopkins, in *2005 IEEE Aerospace Conference Proceedings* (2005).

[6] M. Z. Cross, A. Zumdieck, R. Lifshitz, and J. L. Rogers, Phys. Rev. Lett. **93**, 224101 (2004).
 [7] J. A. Acebrón, L. Bonilla, C. J. P. Vicente, F. Ritort, and R. Spigler, Rev. Mod. Phys. **77**, 137 (2005).
 [8] M. Golubitsky and I. Stewart, *The Symmetry Perspective: From Equilibrium to Chaos in Phase Space and Physical Space* (Birkhauser, Boston, 2003).
 [9] M. Golubitsky and I. Stewart, in *Equadiff 2003: Proceedings of the International Conference on Differential Equations*, edited by F. Dumortier, H. W. Broer, J. Mawhin, A. Vanderbauwhede, and S. M. V. Lunel (World Scientific, Singapore,

- 2005), pp. 13–24.
- [10] J. L. Rogers, S. Peleš, and K. Wiesenfeld, *IEEE J. Quantum Electron.* **41**, 767 (2005).
- [11] T. H. Maiman, *Nature (London)* **187**, 493 (1960).
- [12] J. E. Ripper and T. L. Paoli, *Appl. Phys. Lett.* **17**, 371 (1970).
- [13] H. Bruesselbach, D. C. Jones, M. S. Mangir, M. Minden, and J. L. Rogers, *Opt. Lett.* **30**, 1339 (2005).
- [14] M. Minden, H. W. Bruesselbach, J. L. Rogers, M. S. Mangir, D. C. Jones, G. J. Dunning, D. L. Hammon, A. J. Solis, and L. Vaughan, *Proc. SPIE* **5335**, 89 (2004).
- [15] V. A. Kozlov, J. Hernandez-Cordero, and T. F. Morse, *Opt. Lett.* **24**, 1814 (1999).
- [16] A. Shirakawa, T. Saitou, T. Sekiguchi, and K. Ichi Ueda, *Opt. Express* **10**, 1167 (2002).
- [17] D. Sabourdy, Y. Kermene, A. Desfarges-Berthelemot, L. Lefort, A. Barthklemly, C. Mahodaux, and D. Pureur, *Electron. Lett.* **38**, 692 (2002).
- [18] J. L. Rogers, M. Minden, and H. Brusselbach, in *The 7th Experimental Chaos Conference* (2002).
- [19] I. B. Schwartz and T. Erneux, *SIAM J. Appl. Math.* **54**, 1082 (1994).
- [20] T. W. Carr, L. Billings, I. B. Schwartz, and I. Triandaf, *Physica D* **147**, 59 (2000).
- [21] F. Fontana, M. Begotti, E. M. Pessina, and L. A. Lugiato, *Opt. Commun.* **114**, 89 (1995).
- [22] Q. L. Williams and R. Roy, *Opt. Lett.* **21**, 1478 (1996).
- [23] Q. L. Williams, J. Garcia-Ojalvo, and R. Roy, *Phys. Rev. A* **55**, 2376 (1997).
- [24] H. D. I. Abarbanel and M. B. Kennel, *Phys. Rev. Lett.* **80**, 3153 (1998).
- [25] F. Brunet, Y. Taillon, P. Galarneau, and S. LaRochelle, *J. Lightwave Technol.* **23**, 2131 (2005).
- [26] E. J. Bochove, P. K. Cheo, and G. G. King, *Opt. Lett.* **28**, 1200 (2003).
- [27] T. B. Simpson, A. Gavrielides, and P. Peterson, *Opt. Express* **10**, 1060 (2002).
- [28] S. Peleš, J. L. Rogers, and K. Wiesenfeld, *Proc. SPIE* **5971**, 59710R (2005).
- [29] A. W. Snyder and J. D. Love, *Optical Waveguide Theory* (Chapman and Hall, London, New York, 1983).
- [30] W.-P. Huang, *J. Opt. Soc. Am. A* **11**, 963 (1993).
- [31] In a more general case, when the loss at the output face is not the same for all fibers, the field propagation along the coupling region ($c < z < L$) is described by $e^{iMd} R e^{iM^T d}$, where R is a diagonal matrix whose entries are reflection coefficients at the output face. In our case all reflection coefficients have the same value r , so we can describe coupling in a more compact form as in Eq. (7).
- [32] S. Wang and H. Winful, *Appl. Phys. Lett.* **52**, 1774 (1988).
- [33] R. M. Gray, *Toeplitz and Circulant Matrices* (2002), <http://www-ee.stanford.edu/~gray/toeplitz.html>
- [34] Note that we used the unitarity condition here merely for convenience. If S is not unitary, e.g., $\sum_m S_{nm} = \alpha e^{i\omega}$, where $\alpha \in \mathbb{R}$, a similar fixed point solution can be found with $G_n = \ln(\alpha r)^{-1}$, and field magnitude defined as $R^2 = [G_n^2 + \ln(\alpha r)] / [2(1 - \alpha r)]$.
- [35] D. Tsygankov, Ph.D. thesis, Georgia Institute of Technology, 2005.
- [36] A. E. Siegman, *Resonant Modes of Linearly Coupled Multiple Fiber Laser Structures* (2004), http://www.stanford.edu/~siegman/coupled_fiber_modes.pdf
- [37] M. Octavio, C. B. Whan, and C. J. Lobb, *Appl. Phys. Lett.* **60**, 766 (1992).
- [38] A. Landsberg, K. Wiesenfeld, and G. Filatrella, *Phys. Lett. A* **233**, 373 (1997).